Proceedings of 15th International Marine Design Conference (IMDC-2024)
June 2-6, 2024
Amsterdam, the Netherlands

Application of Sampling Methods for Constrained Space in Hull Form Optimization

HOU Wen-long[1,2]，CHANG Hai-chao[1,2,*]，FENG Bai-wei[1,2]，LIU Zu-yuan[1,2]，ZHAN Cheng-sheng[1,2], CHENG Xi-de[1,2]

ABSTRACT

Use of approximation models instead of direct application of CFD tools plays a crucial role in hull form optimization to enhance efficiency. The selection of sample points directly impacts the accuracy and cost of approximation models, and the effectiveness of hull form optimization. This paper presents a sampling method based on constrained space. The distribution pattern of the constrained space is initially analyzed, and its boundary is subsequently extracted by the Support Vector Machine (SVM), providing guidance for the subsequent sample selection. To ensure effective sampling within the constrained space, the maximum minimum distance criterion is employed. The proposed methodology is validated via a case study involving a 13,000DWT inland twin-screw bulk carrier. The Kriging approximation model is constructed to optimize the hull form while adhering to specific constraint conditions, thereby demonstrating the feasibility and efficacy of the proposed approach.

KEY WORDS

Hull Form Optimization; Constrained Space; Support Vector Machine; Maximum Minimum Distance Criterion.

INTRODUCTION

At present, ship shape optimization based on approximate model has garnered significant attention. Utilizing an approximation model, instead of a higher-accuracy simulation model, during the ship optimization process serves to reduce computational complexity and enhance optimization efficiency. Wang et al. (2018) introduced the Kriging approximation model in the multi-objective fast optimization process of container ship (KCS) and combined it with the non-dominated genetic algorithm (NSGA-II) to complete the resistance optimization objective for KCS ship under design draft and service speed, and at the same time, improve the ship's wave resistance and optimization efficiency. Liu et al. (2022) constructed a multi-fidelity Co-Kriging agent model, and illustrated the advantages of multi-fidelity Co-Kriging agent model compared with single-fidelity Kriging agent model in terms of fidelity and efficiency through a series of numerical examples. Finally, the ship shape optimization design for the total hull drag of DTMB-5415 at the design speed is given. Chen et al. (2015) optimized the hull shape of a high-speed Delft catamaran to reduce the drag based on the idea of dimensionality reduction in the design space and geometrical variability assessment by means of the Karhunen-Loève unfolding, approximate modeling, and deterministic Particle Swarm Optimization (PSO), compared with the previous optimization process Compared with the previous optimization process, the computational cost is reduced by 90% and the drag is further reduced by 6.6%. Bonfiglio et al. (2018) used multi-fidelity gaussian process regression (MF-GPR) to build a probabilistic approximation model and explored the 35-dimensional SWATH hull-shape optimization and 17-dimensional underwater wing-shape optimization, respectively, which greatly reduced the optimization and computational workload. In order to further improve the accuracy of the approximation model, Hochkirch et al. (2013) studied the Hybrid Model (HM).

[1] School of Naval Architecture, Ocean and Energy Power Engineering, Wuhan University of Technology, Wuhan 430063, China
[2] Key Laboratory of High Performance Ship Technology (Wuhan University of Technology), Ministry of Education, Wuhan 430063, China
[*] Correspondence: 361169473@163.com

Submitted: 12 February 2024, Revised: 13 April 2024, Accepted: 1 May 2024, Published: 18 May 2024

Conference paper, DOI: https://doi.org/10.59490/imdc.2024.832 e-ISSN: 3050-4864

Before constructing the approximation model, a certain number of sample points need to be selected in the design space for CFD calculation, and subsequently they will be used as the training set for constructing the approximation model. Currently, the common sampling methods used in ship optimization are as follows: orthogonal design, Latin square design, uniform design, sobol random sampling and so on. On the basis of these commonly used methods, many scholars have conducted a large number of detailed studies. Ouyang et al. (2022) proposed a maximum entropy adaptive sampling method based on uniform experimental design. By comparing with the incremental Latin hypercube-based method, the adaptive sample distribution obtained by the proposed method is more uniform and the global approximation model is more accurate. Chang et al. (2021) proposed a dynamic sampling method (DSM) to improve the accuracy and efficiency of the approximation model by taking into account the effect of sample quality measurements in the input and output parameter spaces. The proposed method is compared with the conventional sampling method, and it is proved that the DSM outperforms the static sampling method. Wang et al. (2021) comparatively analyzed the hydrodynamic performance of a smooth boat in the mono-hull state (MFS) and the three-hull state (TFS), and the optimal range of the sideboard arrangement is given by using the full factorial design space sampling method, which is verified on the scale of a real boat. Based on the LHD sampling method, Wang et al. (2021) analyzed the prediction accuracy of the SVR model with different sample set sizes, and completed the multi-objective optimization of drag and companion flow of offshore aquaculture vessels. Feng et al. (2018) also optimized the hull profile and jet conduit shape of a water-jet propelled trimaran based on the LHD sampling method.

The above studies on approximate modeling and sampling methods seek to make the samples fill the entire design space uniformly, while the limitations of the constraints are not considered. This means that the sample set we obtain through the above sampling methods will contain both sample ship types that satisfy the constraints and sample ship types that do not satisfy the constraints, leading to a decrease in the accuracy of the model forecasts. Therefore, if the constraints can be considered at the sampling stage, and the sample point sets satisfying the constraints can be obtained directly through the sampling method, avoiding the mixing of sample ship types satisfying the constraints and those not satisfying the constraints to the maximum extent, it will be conducive to the construction of the subsequent approximate model and optimization algorithms, which will improve the forecast accuracy of the approximate model and at the same time, save the time cost of optimization.

This paper focuses on a 13,000DWT inland twin-screw bulk carrier, considering the total ship resistance as the optimization objective. The paper employs the constraint-space oriented sampling method proposed herein to construct a Kriging approximation model. A comparative study is conducted on the optimization of the ship type under specified constraint conditions.

SAMPLE POINT SELECTION METHOD FOR CONSTRAINT SPACE

To incorporate constraints into the sampling stage and achieve the goal of directly obtaining a set of sample points that satisfy the constraints through sampling, this paper introduces a sample point selection method based on the support vector machine in the constraint space. The workflow is illustrated in Figure 1. The specific process is as follows:

(1) The range of variation of the variables is first determined to form the initial design space;

(2) Sampling in Design Space;

(3) The constraints on the sample points are calculated to complete the data preparation for partitioning the initial design space;

(4) The initial design space is partitioned using the support vector machine method to obtain the space we need to satisfy the constraints;

(5) If the number of sample points in the feasible space that satisfies the constraints is sufficient, these sample points can be used for the construction of the approximation model, otherwise, new sample points have to be co-opted in the feasible space that satisfies the constraints until the requirement of the number of sample points for the construction of the approximation model is met.

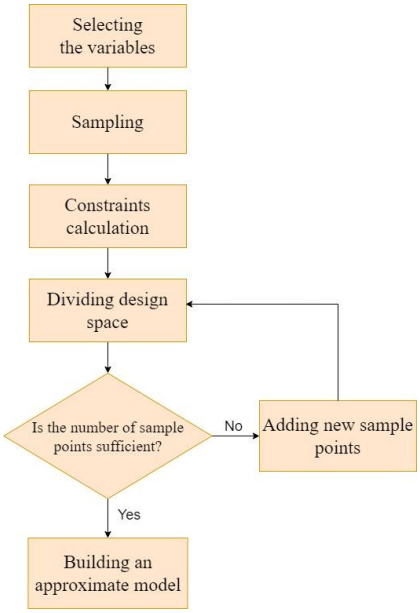

Figure 1: Constraint space oriented approximation model construction process.

As can be seen, the core of the method is the delineation of the design space and the selection of subsequent sample points, which are described below respectively.

Support Vector Machine Algorithm Principles

The SVM algorithm is a machine learning method based on statistical learning theory, which aims to find the "optimal hyperplane" that can effectively classify the training samples. In most cases, this "optimal hyperplane" should have the best robustness to local perturbations in the training samples, while having the smallest classification error and the strongest ability to generalize to unseen examples.

Suppose that for a given training set is as follows:

$$\{(x_1, y_1), (x_2, y_2), \cdots, (x_n, y_n)\}, \quad x \in R^n, y \in \{1, -1\} \tag{1}$$

The hyperplane can be expressed as $\omega^T x + b = 0$, where $\omega = (\omega_1; \omega_2; \ldots; \omega_d)$ is the normal vector and b is the displacement term. It can be found that the normal vector ω and the displacement b determine a hyperplane, so we can denote a definite hyperplane as (ω, b). In order for a hyperplane to classify all training samples correctly and have a classification interval, it is required to satisfy the following constraints:

$$y_i[(\omega^T \cdot x_i) + b] \geq 1 \quad i = 1, 2, \cdots, n \tag{2}$$

As shown in the Figure 2., the closest sample points to the hyperplane such that the equality sign of the constraints holds are the "support vectors", and the sum of the distances of the two dissimilar support vectors to the hyperplane is

$$\gamma = \frac{2}{\|\omega\|} \tag{3}$$

γ is also referred to as the classification interval. In order to maximize the classification interval, the problem of constructing an optimal hyperplane can be transformed into solving the following equation under constraints:

$$\begin{cases} \min\limits_{\omega,b} \dfrac{1}{2}\|\omega\| \\ s.t.\ y_i[(\omega^T \cdot x_i)+b] \geq 1 \end{cases} \quad [4]$$

Using the Lagrange factorization method and the dyadic principle, the above equation can again be transformed into the following optimal classification function problem:

$$f(x) = sign[\sum_{i=1}^{n} \alpha_i y_i \langle x_i, x \rangle + b] \quad [5]$$

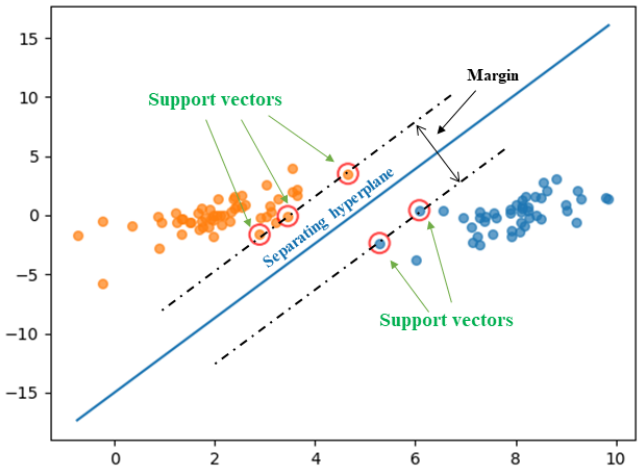

Figure 2: Optimally separating hyperplane and support vectors.

If the data are nonlinearly differentiable, SVM first maps the input space to a high-dimensional linearly differentiable space through the kernel function, and then classifies in the new space. In addition, the outliers in the data will seriously affect the classification performance of SVM, in order to make the model more robust, the soft interval and penalty term are introduced, and the improved SVM objective function is as follows:

$$\begin{cases} \dfrac{2}{\|\omega\|} \min\limits_{\omega,b} \dfrac{1}{2}\|\omega\| + C\sum\limits_{i=1}^{n} \xi_i \\ s.t.\ y_i(\omega^T x_i + b) \geq 1-\xi,\ \ \xi_i \geq 0,\ C \geq 0 \quad i = 1, 2, \cdots n \end{cases} \quad [6]$$

In the above equation, C is the penalty coefficient to control the misclassification of outliers, the larger C means the stricter, the lower tolerance for outliers; on the contrary, it means the more lenient, the higher tolerance for outliers. The classification function of SVM in the case of kernel mapping is:

$$f(x) = sign[\sum_{i=0}^{n} a_i y_i K\langle x_i, x \rangle + b] \quad [7]$$

In the above equation, $K\langle x_i, x \rangle$ is the kernel function. The commonly used kernel functions are polynomial kernel function, Gaussian radial basis kernel function and Sigmoid kernel function.

Dividing the Design Space

In this paper, SVM method is utilized to divide the design space to get the corresponding form of constraint space, the basic division process is shown in Figure 3., and the specific division process is as follows:

Step 1: The sample point set that completes the calculation of constraints is filtered and divided into samples that satisfy the constraints and samples that violate the constraints, forming the sample point set respectively. And then the whole sample set is divided into training set and testing set according to a certain proportion.

Step 2: Preliminarily, the penalty coefficient C and other related parameters of the SVM model are selected, the Gaussian kernel function is selected as the kernel function of the SVM, and the kernel function parameters, which will affect the number of support vectors and the dispersion of the sample features.

Step 3: The training samples are classified and the relevant parameters of the SVM are adjusted appropriately according to the accuracy of the classification.

Step 4: Finish training the SVM model and save the model output.

With the SVM algorithm, it is possible to divide the region occupied by feasible and infeasible sample points to obtain a new feasible space that satisfies the constraints, providing a guide for subsequent sampling in the feasible space.

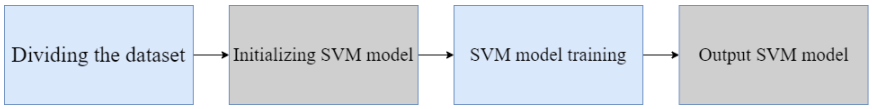

Figure 3: Process of dividing the design space.

Sample Points Selection Method

After dividing the design space by SVM method, we get the feasible space and infeasible space. If the number of sample points in the feasible space is not enough for constructing the approximate model, then we need to select new sample points in the feasible space. The following briefly describes the sample point selection strategy in the feasible space:

First, the existing sample points in the feasible space are formed into a sample point set, and then, starting from the selection of the first point, it is necessary to satisfy the maximization of the minimum distance from each newly selected sample point to the existing sample points. According to the following rule, the sample points are selected sequentially until the number of sample points in the point set meets the required number of inputs (Teng et al., 2018). Denote the minimum distance between any two points as the Euclidean distance:

$$d(x,y)=\|x-y\|_2 \tag{8}$$

The first n sample points that have been selected are $s_1, s_2, \cdots, s_n$, then the set of points is

$$S_n=\{s_1, s_2, \cdots, s_n\} \tag{9}$$

The distance from any sample point x to the set of points S_n is

$$d(x,S_n)=\min\{d(x,s_i)\} \tag{10}$$

The next sample point to be selected is

$$s_{n+1}=\arg\max\{d(x,S_n)\} \tag{11}$$

All sample points in the final point set are widely and uniformly distributed in the feasible space.

Taking the two-dimensional constraint space constituted by inequality [12] as an example, the effect of sample point selection is shown in Figure 4. Where the region constituted by the blue points is the constraint space region, and the red points are the sample points obtained by sampling.

$$\begin{cases} 0\le x\le 10 \\ 0\le y\le 10 \\ x+y\le 10 \end{cases} \tag{12}$$

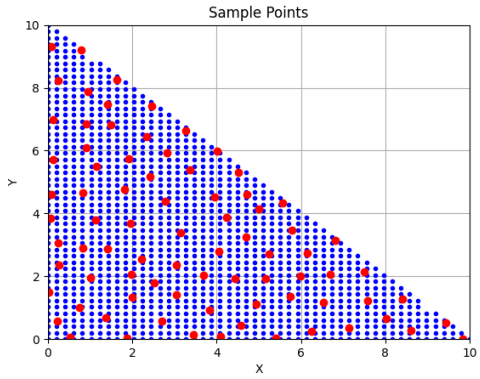

Figure 4: Sample point selection oriented to the constraint space

EXAMPLE

The Optimization Model

Taking the 13,000DWT inland bulk carrier as an example, a three-dimensional parametric model of the ship was constructed in the fully parametric modeling software CAESES, with a scaling ratio of 1:25 (e.g. Figure 5), and its main parameters are shown in Table 1. Three variables to be optimized for the design were selected as b_B, y_b, and area_ratio, and their specific meanings and ranges of variations are shown in Table 2.

Figure 5: 13,000DWT inland waterway twin-screw bulk carrier

Table 1: Main parameters of model ship

L_{pp}	L_{cb}	B	T	C_b	∇	S_{wet}
5.08 *m*	2.564 *m*	0.872 *m*	0.22 *m*	0.86	0.836 m^3	6.018 m^2

Table 2: Design parameters

Design Variables	Design Variable Meaning	Initial Value	Lower Bound	Upper Bound
b_B	Stern Axis Distance Breadth Ratio	0.5287	0.5	0.55
y_b	Bobtail Medial Fullness	0.4162	0.1	0.6
area_ratio	Design Below-Waterline Fullness	0.8356	0.75	0.9

Minimizing the total resistance R of the model ship at the draft of T=0.22m and F_r=0.1457 is taken as the optimization objective.

$$\min f_{obj} = R \quad T=0.22m \quad F_r = 0.1457 \qquad [13]$$

The constraints are listed below:

(1) The optimized displacement must not be less than that of the mother ship, and this constraint is shown in Equation [14]:

$$\frac{\nabla_{opt} - \nabla}{\nabla} \geq 0 \quad [14]$$

(2) The optimized longitudinal position of the buoyant center of gravity of the corresponding structure must not exceed the midship position at 0.55% towards the bow, and this constraint is shown in Equation [15]:

$$\frac{L_{cb} - L_{pp}/2}{L_{pp}} \leq 0.55\% \quad [15]$$

Analysis of the Design Space

According to the upper and lower limits of the three design parameters, 500 sample points are sampled in the design space using the uniform design sampling method, and these 500 sample points correspond to 500 different sample ship types. The hydrostatic calculation module of CAESES is used to calculate the hydrostatic data for these 500 sample points, and the calculated results are compared with the optimized performance constraints of the ship types. The 500 sample points are classified into two categories based on the comparison results: 1. feasible sample points that satisfy the constraints; 2. infeasible sample points that do not satisfy the constraints. Visualize this 3D design space as shown in Figure 6.

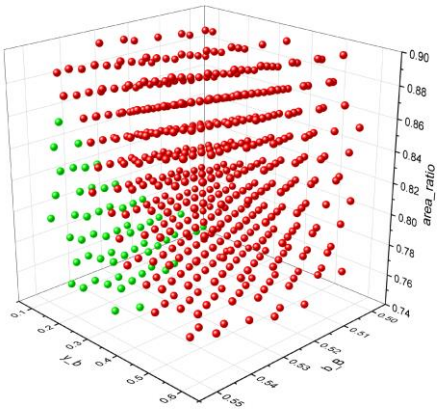

Figure 6: Three-dimensional design space

The red points in Figure 5 indicate infeasible sample points that do not satisfy the constraints, and the green points indicate feasible sample points that satisfy the constraints. From the figure, it can be seen that most of the sample points obtained after sampling according to the original design parameter variation range do not satisfy the performance constraints, and only a small number of feasible sample points satisfy the performance constraints and are distributed in the corner of the design space, so constructing an approximation model based on the whole set of sample points will cause a big trouble to the optimization work.

Optimization Strategies

Optimization Processes

After obtaining the feasible space, the number of sample points distributed within it is 71 in total, which does not meet the demand for the number of samples for constructing the approximation model, and it is necessary to increase the number of sample points in the feasible space to 80, and use the sample point selection method based on the maximum-minimum distance to increase the sample points by 9 sample points in the feasible space. Some of the selected sample points are shown in Table 3 below:

Table 3: Selected sample points co-opted in the feasible space

Number	b_B	y_b	area_ratio
1	0.5500	0.1256	0.8154
2	0.5423	0.1641	0.7500
3	0.5500	0.3051	0.7731
4	0.5436	0.1128	0.7615
5	0.5498	0.2154	0.8000
6	0.5449	0.1641	0.7962
7	0.5487	0.2026	0.7615
8	0.5346	0.2795	0.7500
9	0.5415	0.1256	0.7885

And then the total resistance of these 80 sample ship types is calculated by STAR-CCM+ software to get the sample set for training the approximation model. Then the Kriging approximation model is constructed and the optimization solver is set up, and the genetic algorithm is chosen for optimization. Finally, the study on the hydrodynamic performance line optimization of this ship is completed.

The constraint space-oriented sampling method proposed in this paper and the traditional method based on uniform test design are simultaneously applied to optimize the hull profile, and the optimization effects of the two methods are compared, and the basic flow of the two methods is shown in Figure 7.

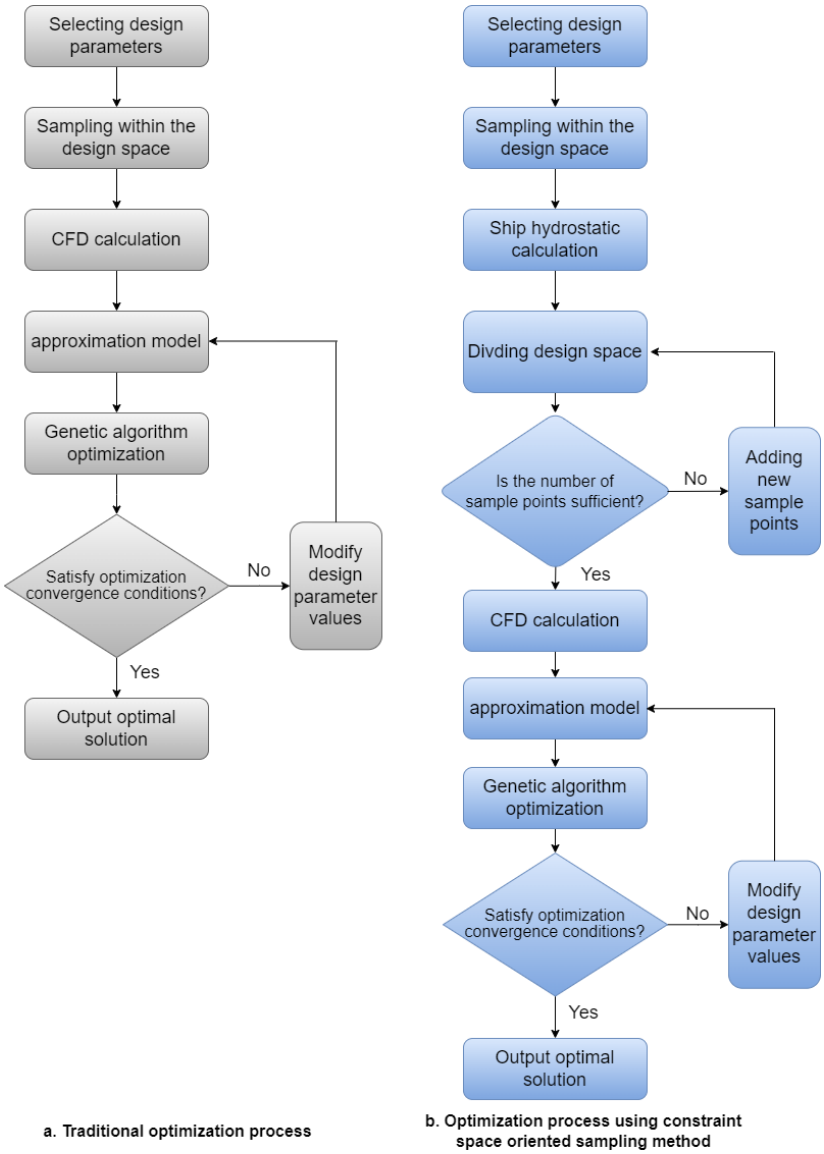

Figure 7: Optimization process

In order to compare the accuracy of the approximate models constructed by the two methods, five sample points are re-selected in the feasible space using the Latin hypercubic sampling method, and the total resistance value is calculated for each sample ship type using the STAR-CCM+ software as the corresponding prediction sample set, and these samples are shown in Table 4. The prediction sample set was forecasted using the Kriging approximation model constructed through two different methods. Finally, the forecasting results of the approximate models constructed by the two methods are evaluated using the root mean square error (RMSE), and the evaluation results are shown in Table 5.

Table 4: Sample points used for assessment

b_B	y_b	area_ratio	Traditional optimization method	Constraint space-oriented optimization method	CFD calculation results
0.5465	0.215	0.7875	14.003 N	13.964 N	13.974 N
0.5395	0.175	0.7815	13.802 N	13.835 N	13.826 N
0.5405	0.125	0.7785	13.873 N	13.832 N	13.793 N
0.5375	0.235	0.7575	13.793 N	13.801 N	13.806 N
0.5415	0.295	0.7725	14.015 N	14.027 N	14.039 N

Optimization Results Analysis

Taking the CFD calculation result as the real drag value of the ship model, the prediction error of the drag and the computational cost of the approximate models constructed by the two methods are compared as shown in Table 5. From the table, it can be seen that the prediction error of the constructed Kriging approximation model is smaller and the prediction accuracy is higher compared with the traditional optimization process after using the method proposed in this paper. This is because the optimization process based on the constraint-space oriented sampling method excludes the sample points that do not satisfy the constraints in the process of constructing the approximation model, which improves the forecast accuracy; On the other hand, using the method proposed in this paper has a lower CFD computational cost, i.e., the number of training samples required to achieve the same accuracy of the approximation model as the traditional method is lower, which is also due to the fact that we only select the sample points that satisfy the constraints to perform the CFD computation and construct the approximation model.

Table 5: Comparison of the accuracy and computational cost

	RMSE	RMSE Comparison	The number of samples for modeling that need to be calculated by CFD
Uniform Design	0.0414	——	500
Constrained Space Sampling Optimization	0.0193	-53.4%	80

Comparison of the bow and stern profiles of the optimized ship and the initial ship obtained after optimization using the two methods can be seen in Figure 8, and it can be seen that some of the ship's profiles have changed to different degrees before and after optimization. As can be seen from the waveforms in Figure 9, the amplitude of the rising wave of both optimized ships is reduced to some extent after optimization compared with the initial ship.

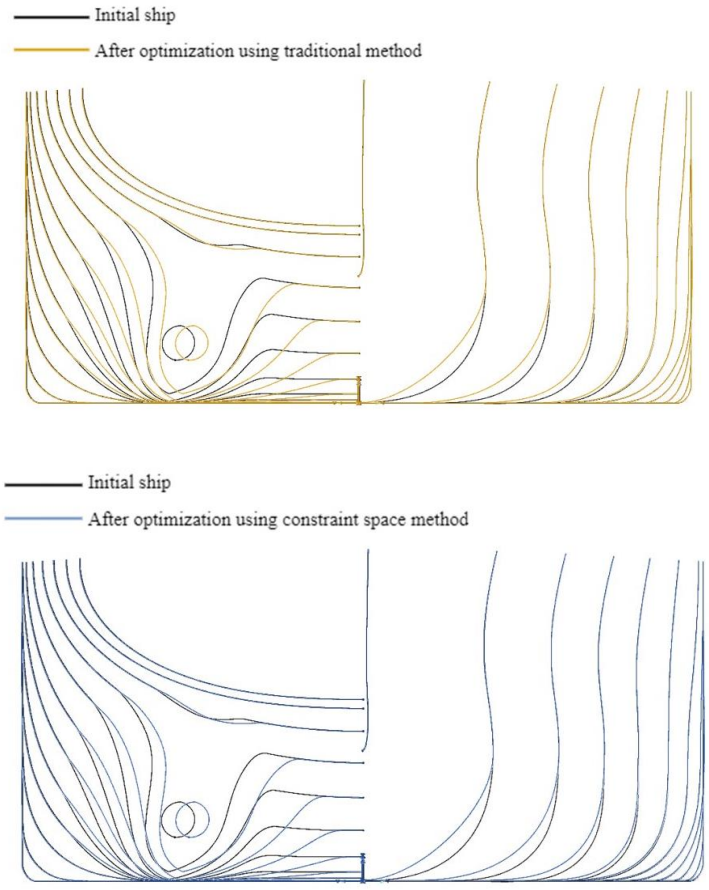

Figure 8: Comparison diagram of the hull lines

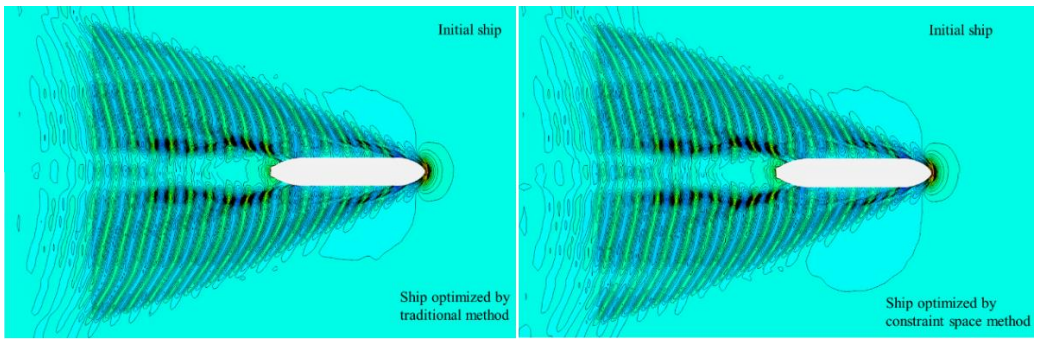

Figure 9: Comparison of waveforms

Comparison of the hydrostatic data of the ship model optimized by the two methods is shown in Table 6. From the hydrostatic data, the displacement volume of the ship model optimized for constraint-oriented spatial sampling increases by 0.23% compared to the initial ship. The longitudinal position of the center of gravity is shifted to the stern direction by 0.001 m compared with the initial ship, and its wet surface area is reduced by 0.75% compared with the initial ship. The drainage volume of the optimized ship model sampled by the traditional uniform design method increased by 0.39% compared to the initial ship, the longitudinal position of the center of buoyancy shifted by 0.003m in the aft direction compared to the initial ship, and the wet surface area decreased by 0.50% compared to the initial ship. It indicates that the frictional resistance of the ship models optimized using both methods has been reduced to different degrees.

The comparison of the drag optimization results of the two methods is shown in Table 7. The total drag of the ship model optimized by the constraint-oriented spatial sampling method is 13.778 N, which is a decrease of 3.35% in the total drag compared with the initial ship, and the error of the approximate model forecast is 0.36%; the total drag of the ship model optimized by the traditional uniform design method is 13.876 N, which is a decrease of 2.66% in the total drag compared with the initial ship, and the error of the approximate model forecast is 0.36%. The approximate model prediction error is 0.36%. Through comparison, it can be found that the approximate model constructed by the constraint space-oriented sampling method proposed in this paper has higher optimization accuracy and better optimization effect.

Table 6: Hydrostatic data

	Drainage volume ∇ (Percentage change)	Longitudinal position of the floating center L_{cb} (Magnitude of change)	Wetted surface area S_{wet} (Percentage change)
Mother ship	0.836 m^3	2.564 m	6.018 m^2
Uniform Design	0.8393 m^3 (+0.39%)	2.561 m (-0.003m)	5.988 m^2 (-0.50%)
Constrained Space Sampling Optimization	0.838 m^3 (+0.23%)	2.563 m (-0.001 m)	5.973 m^2 (-0.75%)

Table 7: Ship model drag optimization results

	Approximate model forecast values	CFD calculated values	Resistance reduction ratio
Mother ship		14.225 N	
Uniform Design Optimization	13.613 N	13.876 N	-2.66%
Error	1.90%		
Constrained Space Sampling Optimization	13.728 N	13.778 N	-3.35%
Error	0.36%		

CONCLUSIONS

This paper proposes a constraint space oriented sampling method in ship shape optimization, taking an inland river 13,000-ton double-tailed bulk carrier as the optimization object, using the method to select the sample points meeting the constraints to construct the approximation model, and using the optimization algorithm to search for the optimal in the feasible space, and finally completing the research on the application of the constraint space oriented sample point selection method in the line shape optimization of this ship. The conclusions are as follows:

(1) The constraint space-oriented sampling method proposed in this paper can improve the forecasting accuracy of the constructed approximate model and save the time cost of calculation.

(2) The application of the constraint space-oriented sampling method to the hydrodynamic performance line shape optimization study of an inland double-tailed bulk carrier, and the comparison with the optimized ship obtained by using the uniform experimental design optimization, shows that the application of this method to the ship shape optimization is feasible.

List of abbreviations

Abbreviations	Explanations
SVM	Support Vector Machine
DWT	Dead Weight Tonnage
L_{pp}	The length between perpendiculars
L_{cb}	The longitudinal center of buoyancy
B	The ship's breadth
T	The ship's draught
C_b	The block coefficient
∇	The volume of displacement
S_{wet}	The wetted surface area
Fr	Froude number
R	The total resistance

CONTRIBUTION STATEMENT

HOU Wen-long: conceptualization, methodology, validation, formal analysis, data curation; **CHANG Hai-chao:** conceptualization, methodology, validation, formal analysis; **FENG Bai-wei:** software; **LIU Zu-yuan:** conceptualization, methodology, formal analysis; **ZHAN Cheng-sheng:** software; **CHENG Xi-de:** software. All authors have read and agreed to the published version of the manuscript.

ACKNOWLEDGEMENTS

This research was funded by the Equipment research Joint Fund of Ministry of Education (Young Talents) project [8091B032201], National Natural Science Foundation of China [grant Numbers 51979211, 52271327, 52271330], 111 Project (BP0820028), to which the authors are most grateful.

REFERENCES

Bonfiglio L, Perdikaris P, Vernengo G, et al. Improving swath seakeeping performance using multi-fidelity Gaussian process and Bayesian optimization[J]. Journal of Ship Research, 2018, 62(04): 223-240.

Chang H, Zhan C, Liu Z, et al. Dynamic sampling method for ship resistance performance optimisation based on approximated model[J]. Ships and Offshore Structures, 2021, 16(4): 386-396.

Chen X, Diez M, Kandasamy M, et al. High-fidelity global optimization of shape design by dimensionality reduction, metamodels and deterministic particle swarm[J]. Engineering Optimization, 2015, 47(4): 473-494.

Feng Y, Chen Z, Dai Y, et al. Multidisciplinary optimization of an offshore aquaculture vessel hull form based on the support vector regression surrogate model[J]. Ocean Engineering, 2018, 166: 145-158.

Guo J, Zhang Y, Chen Z, et al. CFD-based multi-objective optimization of a waterjet-propelled trimaran[J]. Ocean Engineering, 2020, 195: 106755.

Hochkirch K, Mallol B. On the importance of full-scale CFD simulations for ships[C]//11th International conference on computer and IT applications in the maritime industries, COMPIT. 2013.

Liu X, Zhao W, Wan D. Multi-fidelity Co-Kriging surrogate model for ship hull form optimization[J]. Ocean Engineering, 2022, 243: 110239.

Ouyang Xuyu, Chang Haichao, Liu zuyuan, et al. Application of Adaptive Sampling Method in Hull Form Optimization[J].Journal of Shanghai Jiao Tong University, 2022,56(07):937-943.

Teng Yiyang, Wu Yun, Xiong Shifeng, et al. A space-filling property of sequential maximin distance designs[J]. Journal of University of Chinese Academy of Sciences,2018,35(06):731-734.

Wang Gangcheng, Ma Ning, Gu Xiechong. Fast Collaborative Multi-Objective Optimization for Hydrodynamic Based on Kriging Surrogate Model[J].Journal of Shanghai Jiao Tong University, 2018,(6): 666-673.

Wang Jiandong, Zhuang Jiayuan, Su Yumin, et al. Inhibition and hydrodynamic analysis of twin side-hulls on the porpoising instability of planing boats(Article)[J].Journal of Marine Science and Engineering, 2021,9(1): 1-26.